JOURNAL OF AGRICULTURAL AND FOOD CHEMISTRY

Article

pubs.acs.org/JAFC

Saffron as a Source of Novel Acetylcholinesterase Inhibitors: Molecular Docking and in Vitro Enzymatic Studies

George D. Geromichalos,*[,†] Fotini N. Lamari,*[,§] Magdalini A. Papandreou,[⊗] Dimitrios T. Trafalis,[⊥] Marigoula Margarity,[⊗] Athanasios Papageorgiou,[‡] and Zacharias Sinakos[△]

[†]Department of Cell Culture−Molecular Modeling and Drug Design, Symeonidion Research Center, Theagenion Cancer Hospital, Thessaloniki, Greece

[§]Laboratory of Pharmacognosy and Chemistry of Natural Products, Department of Pharmacy, University of Patras, Rion 26504, Greece

[⊗]Laboratory of Human and Animal Physiology, Department of Biology, University of Patras, Patras 26504, Greece

[⊥]Department of Pharmacology, Medical School, University of Athens, Athens, Greece

[‡]Department of Experimental Chemotherapy, Symeonidion Research Center, Theagenion Cancer Hospital, Thessaloniki, Greece

[△]Honored Professor of Haematology, Medical School, Aristotle University of Thessaloniki, Thessaloniki, Greece

Supporting Information

ABSTRACT: Inhibitors of acetylcholine breakdown by acetylcholinesterase (AChE) constitute the main therapeutic modality for Alzheimer's disease. In the search for natural products with inhibitory action on AChE, this study investigated the activity of saffron extract and its constituents by in vitro enzymatic and molecular docking studies. Saffron has been used in traditional medicine against Alzheimer's disease. Saffron extract showed moderate AChE inhibitory activity (up to 30%), but IC_{50} values of crocetin, dimethylcrocetin, and safranal were 96.33, 107.1, and 21.09 μM, respectively. Kinetic analysis showed mixed-type inhibition, which was verified by in silico docking studies. Safranal interacts only with the binding site of the AChE, but crocetin and dimethylcrocetin bind simultaneously to the catalytic and peripheral anionic sites. These results reinforce previous findings about the beneficial action of saffron against Alzheimer's disease and may be of value for the development of novel therapeutic agents based on carotenoid-based dual binding inhibitors.

KEYWORDS: *acetylcholinesterase, dual inhibitors, in silico, saffron, mixed inhibition, crocetin, safranal*

INTRODUCTION

Alzheimer's disease (AD) is a multifactorial dementia characterized by cerebral accumulation of extracellular amyloid-β (Aβ) protein aggregates (senile plaques) and intraneuronal hyperphosphorylated twisted filaments of tau protein (neurofibrillary tangles) in brain areas associated with learning and memory (e.g., cortex, hippocampus, nucleus basalis of Meynhert),[1] resulting, thus, in profound memory disturbances and irreversible impairment of cognitive function. The latter was ascribed primarily to the loss of cholinergic neurons in those areas, due to Aβ and tau buildups, and led to the formation of "the cholinergic hypothesis" of AD.[2,3]

The abnormalities in cholinergic metabolism seen in AD are not viewed as the cause of the disorder, but cholinergic involvement is significant because it is universal, correlates with cognitive defects, and is one of the few pathophysiologic phenomena that can be addressed with currently approved treatment options, such as cholinesterase inhibitors (ChEIs) [e.g., tacrine (THA), rivastigmine, and galanthamine (GNT)]. ChEIs enhance cognitive function by inhibiting the catabolism of the neurotransmitter acetylcholine (ACh) by acetylcholinesterase (AChE) increasing the action of ACh in the synapse. Although various clinical studies document the beneficial effects of current AChE inhibitors on cognition and behavior, their benefits are modest, suffer from short half-lives, and show serious side effects caused by activation of peripheral cholinergic systems.[4−6] Potent AChE inhibitors belong to the class of alkaloids, due to the requirement for positively charged quaternary ammonium in the structure, such as GNT and physostigmine.

AChE, apart from its involvement in cholinergic synaptic transmission, is also known to accelerate the aggregation of Aβ during the early stages of AD, primarily via interactions through its peripheral anionic binding site (PAS).[7−9] In light of these data, the search for new AChE inhibitors for AD now includes the search of dual binding molecules, being able to interact simultaneously with both the PAS and the catalytic subsite of AChE.[10−12]

Advances in X-ray crystallography and site-directed mutagenesis have enabled the detailed mapping of AChE's active center. Human AChE (EC 3.1.1.7) is a globular protein containing a 20 Å deep groove (gorge), which includes the following loci: (1) the acyl-binding pocket Phe295(288) and Phe297(290) (values in parentheses represent the amino acid numbering positions in *Torpedo californica* AChE) at the base

Received: February 9, 2012
Revised: May 29, 2012
Accepted: June 1, 2012
Published: June 1, 2012

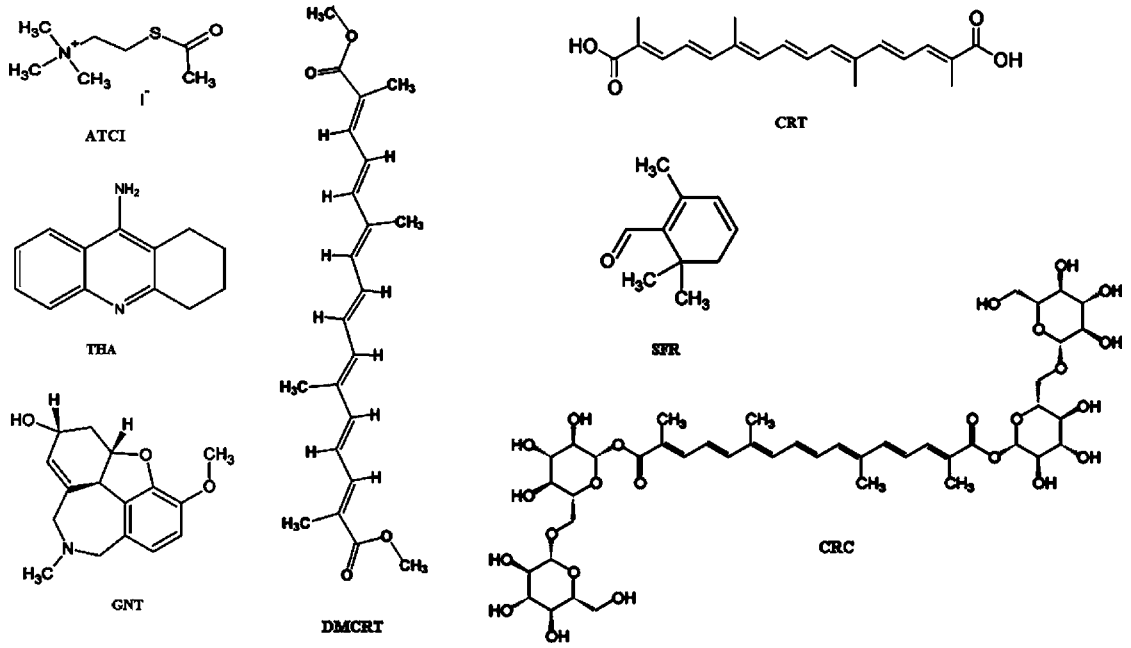

Figure 1. Chemical structures of AChE's substrate (acetylthiocholine, ATCI) and inhibitors (tacrine, THA, and galanthamine, GNT) and saffron's bioactive constituents/metabolites (crocin, CRC; crocetin, CRT; dimethylcrocetin, DMCRT; and safranal, SFR).

of the gorge; (2) the esteratic locus, which consists of two subsites, the oxyanion hole [Gly120(118), Gly121(119), and Ala204(201)] and the active site catalytic serine hydrolase triad [His447(440), Glu334(327), and Ser203(200)]; (3) the quaternary ammonium binding locus [Trp86(84)]; and (4) the PAS site [Tyr72(70), Tyr124(121), and Trp286(279)], situated >10 Å above the active site triad and near the gorge entrance.[13,14]

Saffron, derived from the stigmas of *Crocus sativus*, is a well-known spice with many reputed therapeutic uses, including its use as a tonic, nerve sedative, and antidepressant and its use against dementias.[15,16] Its composition is rare because it is a source of crocins, that is, mono- and diglycosides of crocetin (CRT). We have shown that the extract has powerful antioxidant properties and that the crocin constituents inhibit amyloid aggregation in vitro.[17] After oral consumption of a cup of saffron infusion, CRT is determined in blood plasma as the main metabolite in humans.[18] Administration of saffron extract to aged mice has been demonstrated to counteract age-related memory impairments and improve cerebral antioxidant markers, in addition to the above effects of saffron administration to adult mice of significantly decreased AChE activity.[19] Beneficial effects against scopolamine-induced recognition memory deficits have also been documented in rats.[20−22] In accordance, two recent phase II clinical studies provide preliminary evidence of a possible therapeutic effect of saffron extract in the treatment of patients with mild to moderate AD.[16,23,24] However, the effect of saffron constituents/metabolites on AChE activity has not been studied, despite its promising in vivo effects.

In the present work, in silico molecular docking studies and in vitro enzymatic kinetic studies have been undertaken as an attempt to explore the ability of saffron constituents to act as potent inhibitors of AChE and to elucidate the possible mechanism of action. AChE from electric eel was used because (a) its oligomeric forms are structurally similar to those in AChE of vertebrates, nerve, and muscles[25,26] and (b) it allows molecular modeling studies to be conducted using the coordinates of the published eel AChE X-ray structure, as stated by Khabid et al.[27] The chemical structures of all saffron constituents tested, that is, crocin (CRC), crocetin (CRT), dimethylcrocetin (DMCRT)m and safranal (SFR), as well as of AChE's substrate acetylthiocholin iodide (ATCI) and of AChE known inhibitors THA and GNT, are shown in Figure 1. CRC, a natural carotenoid, is the diester formed by the disaccharide gentiobiose and CRT. CRT is the main metabolite in humans, whereas the synthetic analogue of DMCRT was used to augment the study of carotenoid structure−activity relationships, that is, to investigate the role of CRT carboxyl groups. SFR is a monoterpene aldehyde and the main component of the essential oil of saffron.

MATERIALS AND METHODS

Plant Material and Extraction. Commercially available pure red Greek saffron (stigmas of *C. sativus*) was kindly provided by the Cooperative Association of Krokos in Kozani, in West Macedonia, Greece. Saffron was extracted with methanol/water 1:1 v/v, as previously described.[17] CRT (purity > 98%) was prepared by saponification of saffron extract, whereas DMCRT was prepared by saponification of saffron extract in the presence of methanol, as previously described,[28,29] and its final purity was >98%. SFR (purity > 88%) was purchased from Sigma-Aldrich Corp., St. Louis, MO, USA.

In Vitro AChE Inhibition Assay. The assay for AChE activity was performed with the colorimetric method of Ellman et al.,[30] utilizing ATCI as a substrate and AChE from the electric eel (Sigma-Aldrich Corp.). Briefly, in the 96-well plates were added 50 μL of 50 mM Tris-HCl, pH 8.0, containing 0.1% bovine serum albumin (BSA), 25 μL of the tested samples (0−8 mM CRT, DMCRT, and SFR dissolved in 50 mM Tris-HCl, pH 8.0) or GNT (1−256 μM), 25 μL of 15 mM ATCI (dissolved in water), and 75 μL of 5 mM 5,5′-dithiobis(2-nitrobenzoate) (DTNB) (dissolved in 50 mM Tris-HCl, pH 8.0, 0.1 M NaCl, 0.02 M $MgCl_2 \cdot 6H_2O$). Absorbance was measured at 405 nm after 5 min of incubation at room temperature, in the dark, to subtract these values from the values after AChE addition and correct for nonenzymatic change of reagent absorbance. Then, 25 μL of 0.22 U/mL of AChE from electric eel (dissolved in 50 mM Tris-HCl, pH 8.0, containing 0.1% w/v BSA) was added, and the absorbance was

Table 1. Enzyme Kinetics of the Tested Compounds on AChE Activity[a]

substrate	inhibitor	IC_{50} (μM)	K_m (μM)	V_{max} (μmol/L/min)	K_i (μM)	type of inhibition
ATCI	control		23.01 ± 2.70 (conf interval: 17.0−29.0)	65 ± 3.3		
ATCI	galanthamine (GNT)	1.93 ± 0.05	26.3 ± 3.02 (conf interval: 19.4−33.1)	65 ± 3.3	3.4 ± 0.3	competitive
ATCI	safranal (SFR)	21.09 ± 0.17	18.5 ± 23.9 (conf interval: 9.6−27.4)	27 ± 2.4	90.6 ± 2.0	mixed
ATCI	crocetin (CRT)	96.33 ± 0.11	19.30 ± 2.6 (conf interval: 13.3−25.2)	39 ± 2.2	28.0 ± 2.3	mixed
ATCI	dimethylcrocetin (DMCRT)	107.1 ± 0.11	16.5 ± 1.9 (conf interval: 12.1−21.0)	38 ± 1.8	16.5 ± 2.4	mixed

[a]The values of V_{max}, K_m, and K_i were calculated by monitoring hydrolysis of substrate (ATCI) by AChE at different substrate concentrations (0.125−64 μM) in the presence or absence of samples (mean results of 4 experiments, run in duplicate) (0.15−34 μM).

measured again after 5 min of incubation at room temperature in the dark. GNT (1−32 μM, final concentrations) (Sigma-Aldrich) was used as a reference inhibitor. In all experiments the final organic solvent percentage was never above 6% v/v; control experiments with the same percentage of organic solvent without sample were also conducted, and the values were subtracted. All determinations were carried out at least four times, and in duplicate, at each concentration in 96-well microplates, using a UV−vis microplate reader (Molecular Devices). Results were reported as percentage of inhibition of AChE activity in the absence of inhibitor/tested compounds (positive control). The concentrations of the tested extracts that inhibited the hydrolysis of substrate (ATCI) by 50% (IC_{50}) were determined by GraphPad Prism4.0 (GraphPad Software, Inc., USA) from sigmoidal dose−response curves obtained by plotting the percentage of inhibition (Y) versus the log concentration (x, μM) of the tested samples, using the equation

$$Y = 100/(1 + 10^{(\mathrm{LogIC}_{50} - x)})$$

Kinetic Analysis of AChE Inhibition. Microplate wells were filled with 50 μL of 50 mM Tris-HCl, pH 8.0, containing 0.1% BSA, 25 μL of the tested phytochemicals (0−256 μM CRT and DMCRT and 0−120 μM SFR) or GNT (0−120 μM), 25 μL of AChE (0.22 U/mL), and 75 μL of 3 mM DTNB (dissolved in 50 mM Tris-HCl, pH 8.0, containing 0.1 M NaCl, 0.02 M $MgCl_2 \cdot 6H_2O$). The mixture of enzyme and inhibitor/or samples was mixed, and absorbance was read at 405 nm after 5 min of incubation at room temperature, in the dark. Immediately after addition of the substrate (25 μL ATCI, 1−512 μM concentrations, dissolved in water), the change of absorbance at 405 nm was monitored for 5 min, and the reaction rate was calculated according to the method of Ellman et al.[30] Inhibition studies were analyzed using GraphPad Prism4.0 software. The analysis of the type of inhibition of AChE activity was determined by the Lineweaver−Burk (LB) plot, whereas the kinetic parameters K_m and V_{max} were obtained by curve fitting according to the classical Michaelis−Menten equation. The inhibition constants (K_i) of the tested samples were calculated according to GraphPad Prism v4.0, from linear regression analysis of LB plots (S, hyperbolic; I, hyperbolic mixed model).

In Silico Computational Methods (Molecular Modeling and Docking Calculations). Molecular models of all compounds described in this work were built in 3D coordinates and their best, most stable (lower energy) conformations were detected by geometrical optimization of their structure in the gas phase, as implemented in the Spartan '08 Molecular Modeling program suite (Spartan '08 v. 1.2.0, Wave Function Inc., Irvine, CA, USA). The molecules' structures were initially optimized by conformational search using the Monte Carlo method with the MMFF94 molecular mechanics model. Geometry optimization was accomplished via quantum-chemical calculations by utilizing the ab initio Hartree−Fock method with the 6-31G* basis set.

Docking calculations were carried out via the BioMedCAChe program, which is part of the CAChe package (CAChe WorkSystem Pro version 7.5.0.85, Fujitsu). Docking experiments employed full ligand flexibility and partial protein flexibility focused at the ligand binding site. AChE complex with various inhibitors has provided valuable knowledge of the interactions that mediate inhibitor binding.[31] To identify the molecular determinants responsible for the binding mode of the studied compounds with AChE protein, we used the determined X-ray crystallographic structure of *T. californica* AChE in complex with the AChE inhibitor, THA (PDB accession no. 1ACJ).[32] X-ray structure was obtained from the Brookhaven Protein Data Bank (RCSB Protein Data Bank, operated by the Research Collaboratory for Structural Bioinformatics).[33] The produced compound−protein complexes were ranked by the energy score, including their binding conformations. 3D models of the above protein crystal structures have been developed after the deletion of the cocrystallized bound inhibitor. The docking procedure provides the treatment of ligand flexibility within the protein binding site by means of a four-point chiral pharmacophoric comparison between the ligand and the site. The final output of the docking procedure is a set of solutions ranked according to the corresponding scoring function values, each defined by the 3D coordinates of its atoms and expressed as a PDB file. The accuracy of BioMedCAChe has been shown to successfully reproduce experimentally observed binding modes, in terms of root-mean squared deviation (rmsd). BioMedCAChe provided excellent result as was observed for the low value of rmsd (best docked solution of 0.43 Å) between experimental and docked structures (this is also shown by superimposition of the above structures). The ability to accurately predict the binding conformation of AChE inhibitors, THA and GNT, to AChE, gave confidence that the BioMedCAChe could also predict, with a similar accuracy, the binding conformations of saffron's bioactive constituents utilized in the current study. The PyMol[34] molecular graphics system was used to visualize the molecules and the results of the docking experiments.

Statistical Analysis. Data are presented as the mean ± SE. Statistical analysis was performed with GraphPad Instat 3 software (GraphPad Instat Software, Inc., USA) using the nonparametric Mann−Whitney test ($p < 0.05$). In all tests, a criterion of $p \leq 0.05$ (two-tailed) was considered to be necessary for statistical significance.

RESULTS

In Vitro Effects on AChE Activity. To study if the tested phytochemicals directly inhibit AChE, the effects of saffron extract and of CRT, DMCRT, SFR, and GNT (positive control) on electric eel AChE activity were tested in vitro, and

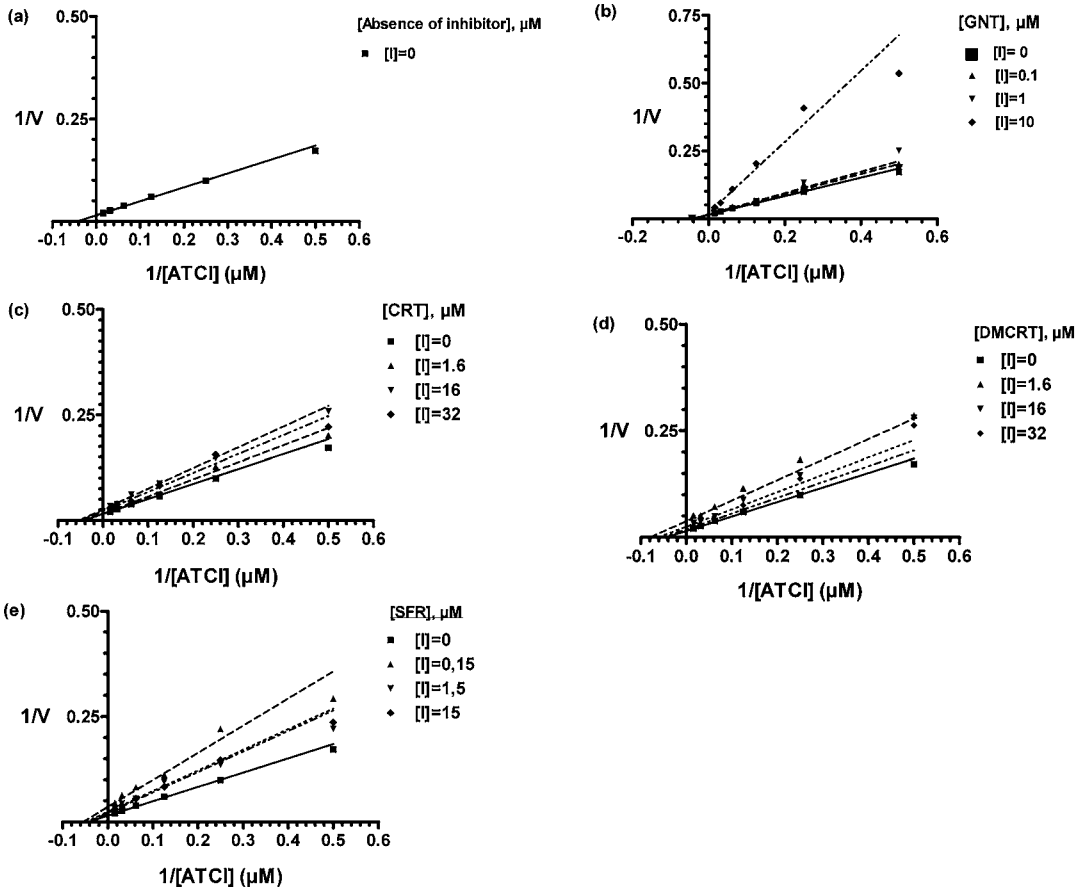

Figure 2. Lineweaver–Burk plots in the absence (a) and presence of standard GNT (b) and saffron's constituents (c–e): $1/V_{max}$ versus 1/[ATCI].

the results are presented in Table 1 and in Figure 3 in the Supporting Information. Saffron showed moderate AChE inhibitory activity (up to 30%). Dose-dependent inhibition of AChE was observed for GNT (Figure 3a of the Supporting Information), a standard AChE inhibitor, with an IC_{50} of 1.93 μM, as well as for the pure compounds, in the order SFR > CRT ≥ DMCRT (Figure 3c–e in the Supporting Information). The determined IC_{50} value of GNT is in agreement with previous results.[31,33]

To elucidate the mechanism of AChE inhibition, kinetic studies of enzyme activity were performed. The relationship between substrate concentration and reaction velocity was in good agreement with Michaelis–Menten kinetics. In the absence of inhibitors, the average K_m for the substrate (ATCI) was 23.01 ± 2.70 μM. When the slopes or the intercepts in the Lineweaver–Burk plots were drawn in GraphPad Prism 4.0 as a function of inhibitor concentration and the kinetic standards determined (Figure 2), CRT, DMCRT, and SFR showed mixed-type inhibition; the α values of CRT and DMCRT are indicative of a mixed-type, uncompetitive inhibition, whereas the α values of SFR show a mixed-type competitive inhibition (Table 1).

In Silico Protein–ligand Docking Study. In silico molecular docking studies were also undertaken to gain insight into the interaction of CRT, DMCRT, CRC, and SFR with the residues of the ligand binding site of the AChE protein and to investigate the underlying mechanism(s) of action(s). The docking simulation studies on the crystal structure of target protein AChE aimed to explore the ability of the studied compounds to act as potent inhibitors of the AChE enzyme. The topography of the calculated binding sites of the studied compounds provides a clearer understanding of their potency differentiation in the inhibition of AChE.

The global energy of interaction (in kcal/mol) for each docking experiments is given as follows: CRT, −32.24; DMCRT, −36.07; CRC, −30.63; SFR, −18.43; THA, −18.26; ATCI, −19.65; and GNT, −32.89. The ligand binding contacts of best docked poses of the known AChE inhibitors GNT and THA and the AChE substrate, ATCI, with key amino acid residues and water molecules in the active site of AChE, are shown in Tables 2–4 in the Supporting Information.

CRT docked very close to ATCI (at a nearby binding position). Its stabilization to the protein's binding pocket was mainly attributed to its formed hydrophobic contacts (23 total contacts): (a) by the hydrophobic residues Phe284, Phe290 (acyl-binding pocket), Phe330, Phe331, Ile287, Leu358; (b) by the acidic and basic charged polar residues Asp285 and Arg289; and (c) by the polar noncharged residues Tyr121 and Ser286 (Table 5 in the Supporting Information). Additionally, CRT was localized inside the binding cavity, making two hydrogen bond contacts with Tyr121 and Asp285. Water molecule wat634 also contributes to the ligand binding by forming a hydrogen bond with O13 of CRT. The binding contacts of CRT with Phe330 and wat634 were found to be common with those of ATCI, THA, and GNT, whereas Tyr121, Phe331, and the acyl-binding residue Phe290 contributed also to the binding of THA and GNT inhibitors. As illustrated from the ligand binding site architecture (Figure 3), CRT was inserted into the narrow aromatic gorge of the crystal structure of AChE, oriented in a way that the molecule's polyene backbone could

dx.doi.org/10.1021/jf300589c | J. Agric. Food Chem. 2012, 60, 6131–6138

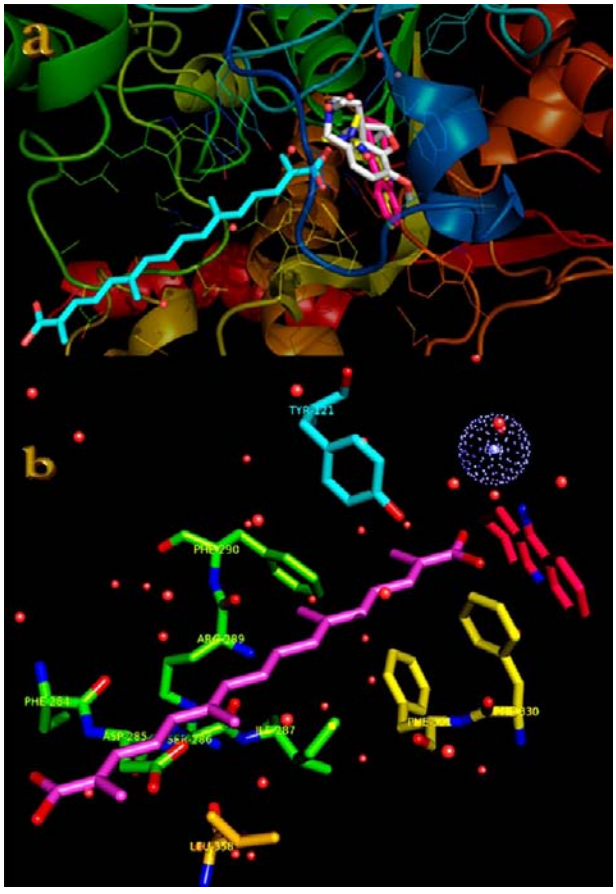

Figure 3. Ligand binding site architecture of AChE target protein (PDB accession no. 1ACJ) with the superimposed docked molecules CRT, ATCI, THA, and GNT. AChE protein is illustrated as a cartoon colored according to chainbow, with additional depiction of selected contacting amino acid residues rendered in line mode (a). The binding envelope of CRT in the target protein (b) is structured with interacting amino acid residues in stick model colored according to chainbow. Interacting water634 molecule is depicted as a blue-dotted sphere. Docked molecules are represented in stick model and colored according to atom type (CRT carbon atoms in light blue (a) or light magenta (b); ATCI, THA, and GNT carbon atoms in yellow, hot pink, and white, respectively). Hydrogen atoms are omitted from all molecules for clarity (final structure was ray traced).

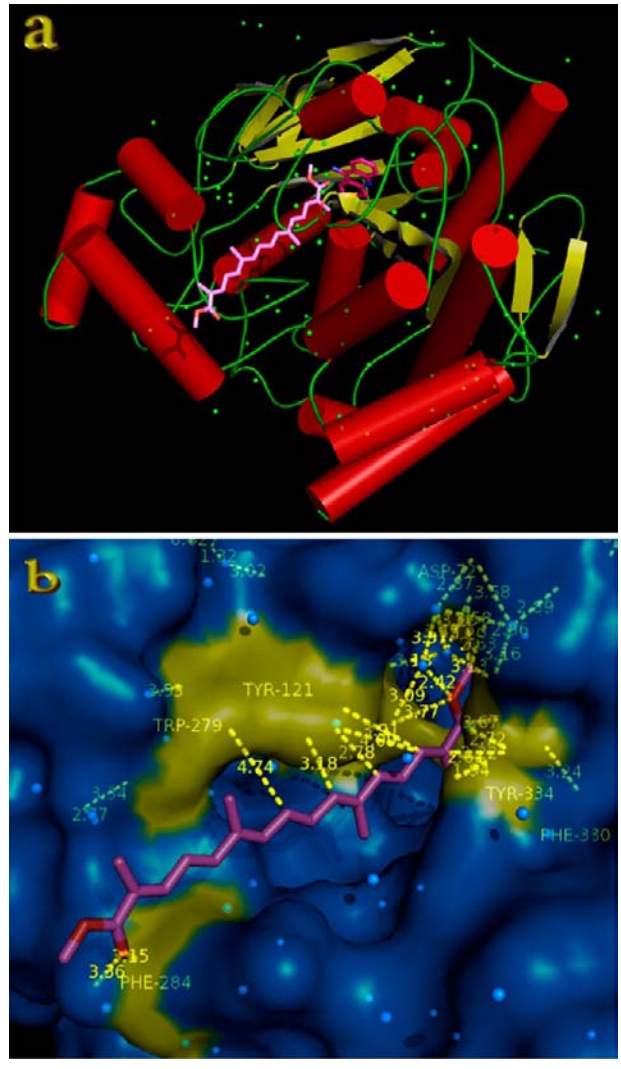

Figure 4. Docking of DMCRT (shown in stick representation and colored according to atom type with light pink C atoms) in the crystal structure of AChE protein cocrystallized with its known inhibitor THA (hot pink C atoms) (PDB accession no. 1ACJ). (a) Target protein is depicted as semitransparent ray-traced cartoon colored by secondary structure (cylindrical helices, red; plank-sheet, yellow; loop, green). A closeup view of the ligand binding pocket is illustrated in semitransparent surface colored by chain (in blue) (b) depicting the binding interactions of DMCRT (light magenta C atoms) with selected amino acid residues in contact highlighted yellow. Hydrophobic and H-bond interactions are shown as dotted lines. Hydrogen atoms are omitted from all molecules for clarity (final structure was ray traced).

be stabilized via hydrophobic contacts with the amino acid residues of the wall of this prolonged cavity. CRT penetrated into the central cavity of the protein, where the catalytic active site is located, with one of its carboxylic ends to be positioned near the catalytic site triad and near the position occupied by ATCI, THA, and GNT. The other end of the molecule (situated near the opening of the aromatic groove at a distance ~20 Å from the catalytic active site) protrudes from the protein's molecule and is stabilized in its position via two H-bond contacts with the amino acid residue Asp285 and the water molecule wat634. Hydrophobic contacts between CRT's atoms of the hydrocarbon skeleton and amino acid residues of the peripheral anionic site contributed further to the attachment of the molecule.

DMCRT superimposed with THA inhibitor is shown in Figure 4 to be anchored inside the ligand binding pocket of the protein. H-bond and hydrophobic interactions between the DMCRT compound and the amino acid residues of the ligand binding cavity of the target protein are shown in Figure 4b. The polyene backbone moiety of the compound is localized inside the anionic binding groove, making contacts with the following amino acid residues: Phe284, Tyr121 (PAS), Trp279 (PAS), and Tyr334. In contrast, Phe330 and Asp72 residues mainly contribute to the attachment of the molecule into the catalytic binding site (Figure 4b). The DMCRT molecule is stabilized in the ligand binding cavity mostly through hydrophobic interactions with residues Asp72, Phe330, Tyr334, Trp279, Phe284, and Asp285 (Table 6 in the Supporting Information). Phe330 was a common binding residue with the ATCI substrate, whereas Phe330 and Tyr121 were common with THA and GNT. The total number of binding contacts found between DMCRT and AChE protein was 21, of which 5 were

dx.doi.org/10.1021/jf300589c | J. Agric. Food Chem. 2012, 60, 6131−6138

H-bonds, 1 was a bridged H-bond, and the rest were hydrophobic.

Docking studies of CRC on AChE demonstrated that the ligand was complexed with the protein with the incorporation of both H-bond and hydrophobic contacts. The docking studies revealed that the CRC molecule anchors inside the aromatic groove, but in a different binding locus from that of THA (binding is stabilized at the peripheral site located at the gorge rim, which encompasses binding sites for allosteric ligands). CRC has a unique orientation along the active-site gorge, extending from the anionic subsite of the active site at the bottom, to the peripheral anionic site at the top, via aromatic stacking interactions with various aromatic acid residues. The superimposed structures of CRC and THA on the target protein are illustrated in Figure 5a. The best possible docking binding mode of CRC was mediated through residues Asn230, His398, Pro232, Asp285, Ser235, and Trp524 and water molecules wat640 and wat650 (11 H-bond contacts) and Arg289, Pro361, Cys357, Asp285, and Phe284 (17 hydrophobic contacts) (Figure 5b; Table 7 in the Supporting Information). No common binding residues with ATCI, THA, or GNT were observed.

The docking procedure positioned SFR into the AChE binding site almost at the same place occupied by THA (Figure 6a,b). Through interaction analysis, it was shown that SFR makes one hydrogen bond contact with the hydroxyl group of wat634, whereas the stabilization of the compound into the pocket was additionally attributed to seven hydrophobic contacts formed by residues Phe330, Gly118, His440, and Trp84 (Figure 6c; Table 8 in the Supporting Information). All binding contacts were found to be common with the corresponding AChE−ATCI/THA complexes, whereas Gly118, His440, and Trp84 were common with the AChE−GNT complex. The former amino acid contacts of SFR are important anchoring residues for the inhibitor and are the main contributors to the inhibitor's interaction. (Data concerning ATCI, GNT, and THA are not shown in the text or tables; they are provided as additional Supporting Information available online.)

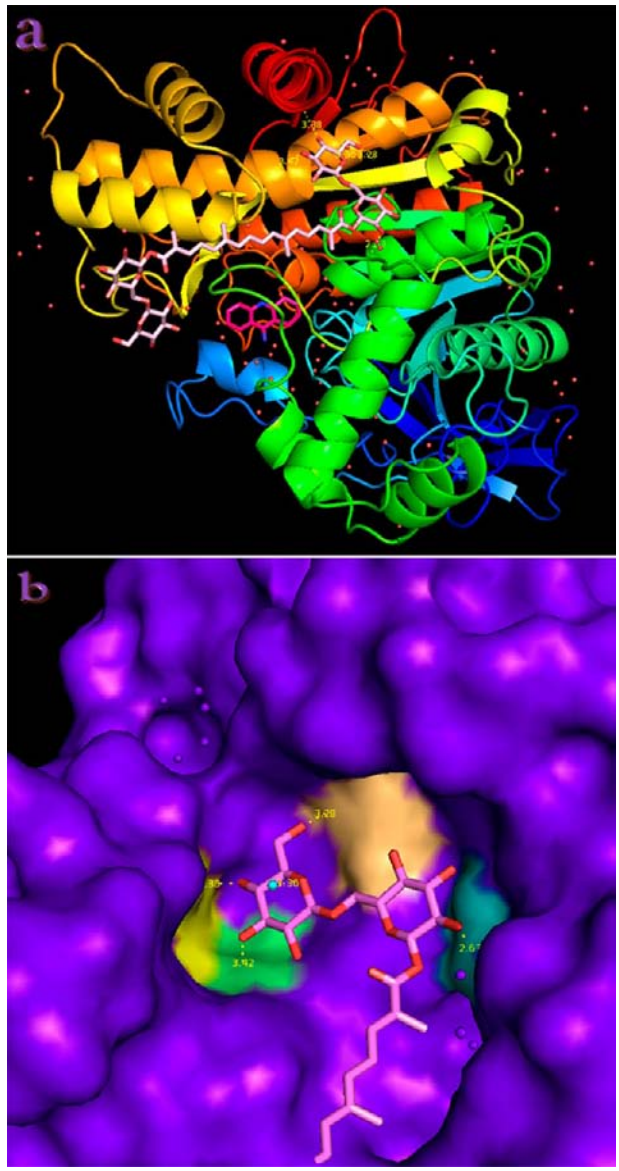

Figure 5. Bound CRC ligand (illustrated in stick mode and colored according to atom type with light pink C atoms) docked in crystal structure of AChE protein (PDB accession no. 1ACJ) depicted as spectrum-colored cartoon (a) or solid surface colored by chain (in purple-blue) with highlighted interacting amino acid residues of the ligand binding cavity (b) in complex with THA (hot pink C). Highlighted residues interacting through H-bond: Asn230, light orange; His398, pale green; Ser235, teal; and Trp524, yellow. Hydrogen-bonded water molecule wat650 is rendered as a light blue sphere. Hydrogen bond and hydrophobic interactions are shown as yellow-dotted lines. Hydrogen atoms are omitted from all molecules for clarity (final structure was ray traced).

DISCUSSION

Our results showed that the crude aqueous methanolic saffron extract exhibited low dose-independent inhibitory values. Analysis of the in vitro effect of CRT, DMCRT, and SFR on AChE inhibition revealed a dose-dependent inhibitory profile, but the IC_{50} values were higher than that of GNT. Kinetic analysis confirmed that GNT exerts a competitive type of inhibition, with a K_i value of 3.36 μM in electric eel enzyme, but the majority of the tested saffron phytochemicals exhibited higher K_i values and a mixed type of inhibition.

Molecular docking studies revealed that CRT and DMCRT were not docked at the same place as ATCI, TCH, and GNT inhibitors, but bound simultaneously to the catalytic and peripheral anionic sites of AChE. CRC, due to its bulky glycosidically linked sugar moieties, was unable to be inserted in depth to the aromatic gorge (did not reach the active site that is found deep in the pocket) and attached to a different locus from that of ATCI, THA, and GNT. The fact that the presence of glycosidically linked sugars alters/impairs binding characteristics might provide an explanation for the rather low inhibitory activity of the saffron extract in vitro. The ability of CRT to span the two "anionic" sites, being ~20 Å apart, and bind to both PAS and the catalytic site of the AChE enzyme opens new possibilities for the design and synthesis of novel dual binding AChE inhibitors, which would beneficially affect cholinergic transmission and Aβ aggregation.

On the other hand, SFR seems to be a more potent inhibitor (IC_{50} = 21.09 ± 0.17, K_i = 90.6 ± 2.0) than the carotenoids, but both kinetic and in silico data show that it completely enters and interacts only with the catalytic center. Similar weak inhibitory action has been reported for many other monoterpenoids,[31] and it is attributed to interactions of the

dx.doi.org/10.1021/jf300589c | J. Agric. Food Chem. 2012, 60, 6131−6138

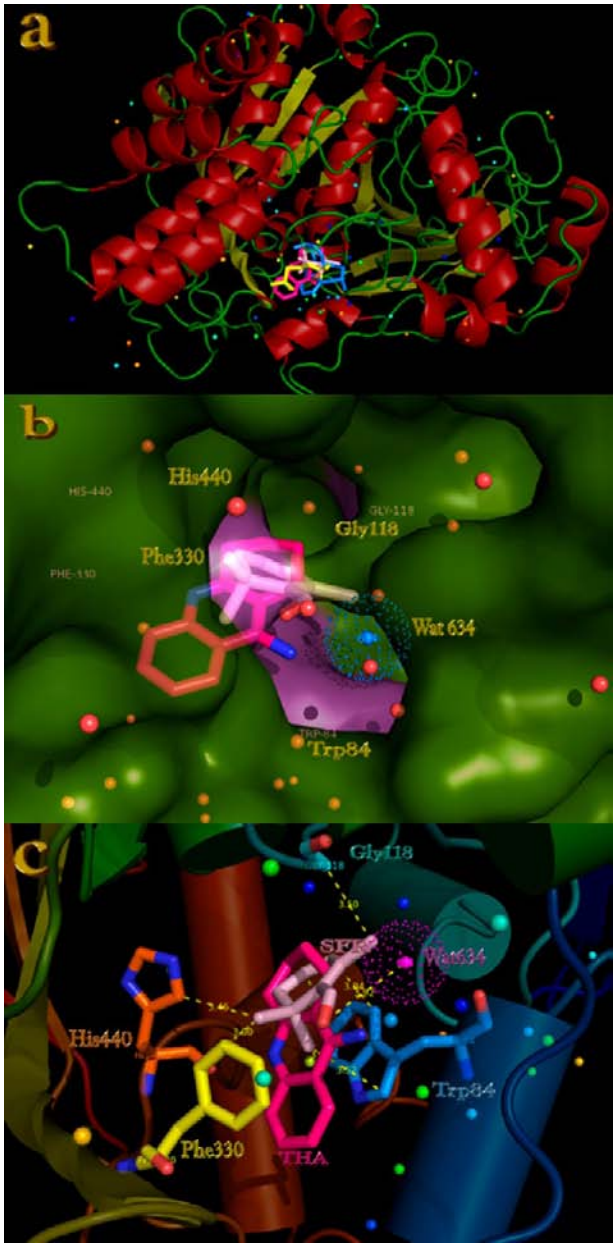

Figure 6. Cartoon diagram (a) of AChE protein with bound SFR molecule in complex with ATCI (rendered as sticks with yellow carbon atoms) and the known inhibitors THA and GNT (rendered as sticks with hot pink and blue carbon atoms, respectively). SFR (depicted as a stick with light pink carbon atoms) is docked into the binding pocket of the protein (illustrated as cartoon colored according to secondary structure) at almost the same place occupied by the cocrystallized THA and GNT inhibitors (PDB ID no. 1ACJ) (dockings of all ligands were performed individually). A closeup view (b) of the ligand binding cavity of the protein is represented as semitransparent surface colored by chain with interacting amino acid residues highlighted in magenta. Wat634 molecule interacting via H-bond with SFR is depicted as a blue-dotted sphere. Interactions of bound SFR and THA ligands (depicted as sticks with light pink and hot pink carbon atoms, respectively) docked in crystal structure of the active site of AChE target protein are colored as chainbow (c). Amino acid residues of the binding pocket are depicted in stick model and colored according to atom type (only the contacts of SFR are shown). The Wat634 molecule is depicted as a magenta-dotted sphere. Hydrogen atoms are omitted from all molecules for clarity (final structure was ray traced).

hydrocarbon skeletal terpenoids with the AChE hydrophobic active center.

The hypothesis derived from the in vitro experiments revealed that the majority of the tested phytochemicals exhibited a mixed type of inhibition, as supported by the adopted in silico studies, where all saffron constituents (apart from SFR) were found to be complexed with the enzyme at a different locus (allosteric binding site) from that of ATCI and the tested inhibitors (THA and GNT). These findings showed, for the first time, that CRT, the main metabolite of CRCs in the living organism, inhibits AChE by binding at two different loci, the catalytic center and the PAS site. This finding may partly explain the beneficial effects of saffron in clinical trials against AD and provides a basis for the design and development of novel pleiotropic AChE inhibitors. The presence of glycosidically linked sugars impairs this activity. Overall, our results showed that the in vitro kinetic analysis, in conjunction with molecular modeling and docking predictions, could be important initial steps toward the development of novel AChE inhibitors.

■ ASSOCIATED CONTENT

Ⓢ Supporting Information

The ligand binding contacts of best docked poses of the known AChE inhibitors GNT and THA, the AChE substrate ATCI, and saffron constituents CRT, DMCRT, CRC, and SFR, with key amino acid residues and water molecules in the active site of AChE, are shown in Tables 2−8. The effectiveness of GNT, saffron, and its constituents in inhibiting AChE activity is shown in Figure 3. IC_{50} or pIC_{50} (when converted to the −log IC_{50} scale) represents the concentration of the tested phytochemical(s) that is required for 50% inhibition in vitro and is calculated by converting the log values back to μM. This material is available free of charge via the Internet at http://pubs.acs.org.

■ AUTHOR INFORMATION

Corresponding Author

*(G.D.G.) Department of Cell Culture-Molecular Modeling and Drug Design, Symeonidion Research Center, Theagenion Cancer Hospital, 2 Al. Symeonidi str., 54007 Thessaloniki, Greece. Phone: +30 231 0898237. Fax: +30 321 0845514. E-mail: geromchem@yahoo.gr. (F.N.L.) Department of Pharmacy, University of Patras, Patras 26504, Greece. Phone:+30 261 0969335. Fax: +30 261 0997714. E-mail: flam@upatras.gr.

Funding

The present study is cofinanced by the EU European Social Fund (80%) and the Greek Ministry of Development-GSRT (20%) and by GlaxoSmithKline.

Notes

The authors declare no competing financial interest.

■ ABBREVIATIONS USED

Aβ, amyloid-β peptide; ACh, acetylcholine; AChE, acetylcholinesterase; AD, Alzheimer's disease; ATCI, acetylthiocholine iodide; BSA, bovine serum albumin; ChAT, choline acetyltransferase; ChEIs, cholinesterase inhibitors; CRC, crocin; CRT, crocetin; DMCRT, dimethylcrocetin; DTNB, 5,5′-dithiobis(2-nitrobenzoate); GNT, galanthamine; PAS, peripheral anionic binding site; PDB, Protein Data Bank; SAR, structure−activity relationship; SFR, safranal; THA, tacrine.

REFERENCES

(1) Ballard, C.; Gauthier, S.; Corbett, A.; Brayne, C.; Aarsland, D.; Jones, E. Alzheimer's disease. *Lancet* **2011**, *377*, 1019−1031.

(2) Perry, E. K. The cholinergic hypothesis—ten years on. *Br. Med. Bull.* **1986**, *42*, 63−69.

(3) Perry, E. K.; Tomlinson, B. E.; Blessed, G.; Bergmann, K.; Gibson, P. H.; Perry, R. H. Correlation of cholinergic abnormalities with senile plaques and mental test scores in senile dementia. *Brain Med. J.* **1978**, *2*, 1457−1459.

(4) Massoud, F.; Leger, G. C. Pharmacological treatment of Alzheimer disease. *Can. J. Psychiatry* **2011**, *56*, 579−588.

(5) Wallin, A. K.; Wattmo, C.; Minthon, L. Galanthamine treatment in Alzheimer's disease: response and long-term outcome in a routine clinical setting. *Neuropsychiatr. Dis. Treat* **2011**, *7*, 565−576.

(6) Lockhart, I. A.; Mitchell, S. A.; Kelly, S. Safety and tolerability of donepezil, rivastigmine and galantamine for patients with Alzheimer's disease: systematic review of the "real world" evidence. *Dement. Geriatr. Cogn. Disord.* **2009**, *28*, 389−403.

(7) Attack, J. R.; Perry, E. K.; Bonham, J. R.; et al. Molecular forms of acetylcholinesterase and butyrylcholinesterase in the aged human central nervous system. *J. Neurochem.* **1986**, *47*, 263−277.

(8) Inestrosa, N. C.; Alvarez, A.; Perez, C. A.; et al. Acetylcholinesterase accelerates assembly of amyloid-β peptides into Alzheimer's fibrils: possible role of the peripheral site of the enzyme. *Neuron* **1996**, *16*, 881−891.

(9) Inestrosa, N. C.; Dinamarca, M. C.; Alvarez, A. Amyloid-cholinesterase interactions. Implications for Alzheimer's disease. *FEBS J.* **2008**, *275*, 625−632.

(10) Colombres, M.; Sagal, J. P.; Inestrosa, N. C. An overview of the current and novel drugs for Alzheimer's disease with particular reference to anti-cholinesterase compounds. *Curr. Pharm. Des.* **2004**, *10*, 3121−3130.

(11) Muñoz-Torrero, D.; Camps, P. Dimeric and hybrid anti-Alzheimer drug candidates. *Curr. Med. Chem.* **2006**, *13*, 399−422.

(12) Muñoz-Torrero, D. Acetylcholinesterase inhibitors as disease-modifying therapies for Alzheimer's disease. *Curr. Med. Chem.* **2008**, *15*, 2433−2455.

(13) Sussman, J. L.; Harel, M.; Frolow, F.; Oefner, C.; Goldman, A.; Toker, L.; Silman, I. Atomic structure of acetylcholinesterase from *Torpedo californica*: a prototypic acetylcholine-binding protein. *Science* **1991**, *253*, 872−879.

(14) Harel, M.; Schalk, I.; Ehret-Sabatier, L.; Bouet, F.; Goeldner, M.; Hirthy, C.; Axelsen, P. H.; Silman, I.; Sussman, J. L. Quaternary ligand binding to aromatic residues in the active-site gorge of acetylcholinesterase. *Proc. Natl. Acad. Sci. U.S.A.* **1993**, *90*, 9031−9035.

(15) Ferrence, S. C.; Bendersky, G. Therapy with saffron and the goddess at Thera. *Perspect. Biol. Med.* **2004**, *47*, 199−226.

(16) Akhondzadeh, S. Herbal medicine in the treatment of psychiatric and neurological disorders. In *Lowcost Approaches to Promote Physical and Mental Health: Theory Research and Practice*; L'Abate, L., Ed.; Springer: New York, 2007; pp 119−138.

(17) Papandreou, M. A.; Kanakis, C. D.; Polissiou, M. G.; Efthimiopoulos, S.; Cordopatis, P.; Margarity, M.; Lamari, F. N. Inhibitory activity on amyloid-beta aggregation and antioxidant properties of *Crocus sativus* stigmas extract and its crocin constituents. *J. Agric. Food Chem.* **2006**, *54*, 8762−8768.

(18) Asai, A.; Nakano, T.; Takahashi, M.; Nagao, A. Orally administered crocetin and crocins are absorbed into blood plasma as crocetin and its glucuronide conjugates in mice. *J. Agric. Food Chem.* **2005**, *53*, 7302−7306.

(19) Papandreou, M. A.; Tsachaki, M.; Efthimiopoulos, S.; Cordopatis, P.; Lamari, F. N.; Margarity, M. Memory enhancing effects of saffron in aged mice are correlated with antioxidant protection. *Behav. Brain Res.* **2011**, *219*, 197−204.

(20) Pitsikas, N.; Boultadakis, A.; Georgiadou, G.; Tarantilis, P. A.; Sakellaridis, N. Effects of the active constituents of *Crocus sativus* L., crocins, in an animal model of anxiety. *Phytomedicine* **2008**, *15*, 1135−1139.

(21) Pitsikas, N.; Zisopoulou, S.; Tarantilis, P. A.; Kanakis, C. D.; Polissiou, M. G.; Sakellaridis, N. Effects of the active constituents of *Crocus sativus* L., crocins on recognition and spatial rats' memory. *Behav. Brain Res.* **2007**, *183*, 141−146.

(22) Pitsikas, N.; Sakellaridis, N. *Crocus sativus* L. extracts antagonize memory impairments in different behavioural tasks in the rat. *Behav. Brain Res.* **2006**, *173*, 112−115.

(23) Akhondzadeh, S.; Sabet, M. S.; Harirchian, M. H.; Togha, M.; Cheraghmakani, H.; Razeghi, S.; Hejazi, S.Sh.; Yousefi, M. H.; Alimardani, R.; Jamshidi, A.; Zare, F.; Moradi, A. Saffron in the treatment of patients with mild to moderate Alzheimer's disease: a 16-week, randomized and placebo-controlled trial. *J. Clin. Pharm. Ther.* **2010**, *35*, 581−588.

(24) Akhondzadeh, S.; Shafiee-Sabet, M.; Harirchian, M. H.; Togha, M.; Cheraghmakani, H.; Razeghi, S.; Hejazi, S. S.; Yousefi, M. H.; Alimardani, R.; Jamshidi, A.; Rezazadeh, S. A.; Yousefi, A.; Zare, F.; Moradi, A.; Vossoughi, A. A 22-week, multicenter, randomized, double-blind controlled trial of *Crocus sativus* in the treatment of mild-to-moderate Alzheimer's disease. *Psychopharmacology (Berlin)* **2010**, *207*, 637−643.

(25) Sussman, J. L.; Harel, M.; Frolow, F.; Oefner, C.; Goldman, A.; Toker, L.; Silman, I. Atomic structure of acetylcholinesterase from *Torpedo californica*: a prototypic acetylcholine-binding protein. *Science* **1991**, *253*, 872.

(26) Bon, S.; Vigny, M.; Massoulie, J. Asymmetric and globular forms of acetylcholinesterase in mammals and birds. *Proc. Natl. Acad. Sci. U.S.A.* **1979**, *76*, 2546.

(27) Khabid, A.; Haq, Z. U.; Anjum, S.; Riaz Khan, M.; Rahman, A. U.; Choudhary, M. I. Kinetics and structure-activity relationship studies on pregnant-type steroidal alkaloids that inhibit cholinesterases. *Bioorg. Med. Chem.* **2004**, *12*, 1995−2003.

(28) Kanakis, C. D.; Tarantilis, P. A.; Tajmir-Riahi, H. A.; Polissiou, M. G. DNA interaction with saffron's secondary metabolites safranal, crocetin, and dimethylcrocetin. *DNA Cell Biol.* **2007**, *26*, 63−70.

(29) Kanakis, C. D.; Tarantilis, P. A.; Tajmir-Riahi, H. A.; Polissiou, M. G. Interaction of tRNA with safranal, crocetin, and dimethylcrocetin. *J. Biomol. Struct. Dyn.* **2007**, *24*, 537−546.

(30) Ellman, G. L.; Courtney, K. D.; Andres, V.; Featherstone, R. M. A new and rapid colorimetric determination of acetyl cholinesterase activity. *Biochem. Pharmacol.* **1961**, *7*, 88−95.

(31) Barril, X.; Orozco, M.; Luque, F. J. Towards improved acetylcholinesterase inhibitors: a structural and computational approach. *Mini Rev. Med. Chem.* **2001**, *1*, 255−266.

(32) Harel, M.; Schalk, I.; Ehret-Sabatier, L.; Bouet, F.; Goeldner, M.; Hirthy, C.; Axelsen, P. H.; Silman, I.; Sussman, J. L. Quaternary ligand binding to aromatic residues in the active-site gorge of acetylcholinesterase. *Proc. Natl. Acad. Sci. U.S.A.* **1993**, *90*, 9031−9035.

(33) Berman, H. M.; Westbrook, J.; Feng, Z.; Gilliland, G.; Bhat, T. N.; Weissig, H.; Shindyalov, I. N.; Bourne, P. E. The Protein Data Bank. *Nucleic Acids Res.* **2000**, *28*, 235−242.

(34) DeLano, W. L. *The PyMOL Molecular Graphics System*; DeLano Scientific: San Carlos, CA, 2002.